HHS Public Access

Author manuscript

Pain. Author manuscript; available in PMC 2019 July 01.

Published in final edited form as:

Pain. 2018 July ; 159(7): 1382–1391. doi:10.1097/j.pain.0000000000001225.

The bivalent ligand MCC22 potently attenuates nociception in a murine model of sickle cell disease

Giuseppe Cataldo[1], **Mary M. Lunzer**[2], **Julie K. Olson**[1], **Eyup Akgün**[2], **John D. Belcher**[3], **Gregory M. Vercellotti**[3], **Philip S. Portoghese**[2], and **Donald A. Simone**[1]

[1]Department of Diagnostic & Biological Sciences, School of Dentistry, University of Minnesota, Minneapolis, MN

[2]Department of Medicinal Chemistry, College of Pharmacy, University of Minnesota, Minneapolis, MN

[3]Department of Medicine, Vascular Biology Center, Division of Hematology, Oncology and Transplantation, University of Minnesota, Minneapolis, MN

Abstract

Sickle cell disease (SCD) is a chronic inflammatory disorder accompanied by chronic pain. In addition to ongoing pain and hyperalgesia, vaso-occlusive crises-induced pain can be chronic or episodic. Since analgesics typically used to treat pain a*re* not very effective in SCD, opioids, including morphine, are a primary treatment for managing pain in SCD but are associated with many serious side effects, including constipation, tolerance, addiction, and respiratory depression. Thus, there is a need for the development of novel treatments for pain in SCD. In this study we used the Townes transgenic mouse model of SCD to investigate the anti-nociceptive efficacy of the bivalent ligand, MCC22, and compared its effectiveness to morphine. MCC22 consists of a mu opioid receptor (MOR) agonist and a chemokine receptor-5 (CCR5) antagonist that are linked through a 22-atom spacer. Our results show that intraperitoneal administration of MCC22 produced exceptionally potent dose-dependent anti-hyperalgesia as compared to morphine, dramatically decreased evoked responses of nociceptive dorsal horn neurons, and decreased expression of pro-inflammatory cytokines in the spinal cord. Moreover, tolerance did not develop to its analgesic effects following repeated administration. In view of the extraordinary potency of MCC22 without tolerance, MCC22 and similar compounds may vastly improve the management of pain associated with SCD.

1. Introduction

Sickle cell disease (SCD) is one of the most common inherited diseases that results from a point mutation in hemoglobin that causes the polymerization of hemoglobin S, giving red blood cells their characteristic sickle shape [18]. Hemolysis, inflammation, oxidative stress,

Corresponding Author: Donald A. Simone, Ph.D., Department of Diagnostic & Biological Sciences, University of Minnesota, School of Dentistry, 515 Delaware St. SE, Minneapolis, MN 55455, Phone: 612-625-6464, Fax: 612-626-2651, simon003@umn.edu.

Conflicts of interest statement

Drs. Vercellotti and Belcher have received research funding from CSL Behring.

vaso-occlusion, and chronic pain are characteristics of SCD [29,45,49]. Vaso-occlusive crises (VOC) can occur in response to inflammation, hypoxic conditions, infections, and surgery. VOC pain can be chronic or episodic, often requiring hospitalizations and analgesics [51]. Opioids, particularly morphine, are commonly used to manage pain in SCD [4,14] but are problematic due to their serious side effects, including tolerance, addiction, and respiratory depression. Thus, there is a need for the development of novel approaches to treat pain in SCD.

Mouse models of SCD allow investigation into mechanisms underlying pain and evaluation of novel therapeutics. HbSS BERK and HbSS Townes mice exhibit robust hyperalgesia to mechanical, heat, and cold stimuli, as well as deep tissue hyperalgesia, which are worsened by hypoxia/reoxygenation [8,31,37]. Sickle mice, like patients, have elevated markers of inflammation including white blood cell counts, serum amyloid P, and cytokines [5]. Electrophysiological studies showed that nociceptors [27,66] and dorsal horn neurons [10] are sensitized in sickle mice. Furthermore, sickle mice exhibited activated astrocytes and microglia in the spinal cord [68].

In the spinal cord, pro-inflammatory cytokines released by glial cells contribute to pain and hyperalgesia, including neuropathic pain [19,42,55,78], by increasing synaptic strength [12] that leads to sensitization of spinal nociceptive neurons [32]. Furthermore, pro-inflammatory cytokines counteract the analgesia produced by opioids [67,70]. One chemokine that is important in spinal nociceptive processing is chemokine ligand 5 (CCL5) and its receptors, including chemokine receptor 5 (CCR5), which have been implicated in neuropathic [38,39,41] and bone cancer [23,24] pain. Functional interactions occur between the mu opioid receptor (MOR) and CCR5 [11,16,36,40,48,58,63] although the precise mechanisms are unclear. One possibility is that this occurs via formation of a heteromer, as evidence exists for heterodimerization of MOR and CCR5 [11,61].

MCC22 was therefore eveloped to target the putative MOR-CCR5 heteromer [2]. The pharmacophores in MCC22 include the mu opioid receptor agonist oxymorphone [72], and the CCR5 antagonist, TAK-220 [64]. These pharmacophores are linked by a 22-atom spacer which confers optimal antinociception in mouse models of inflammatory pain [2]. Its potency was much greater than that of morphine and was several orders of magnitude more potent than any of its homologs with shorter spacers. Also, the fact that MCC22 was ~3600-fold more potent than a mixture consisting of the monovalent mu agonist and the CCR5 antagonist ligand suggest MOR-CCR5 heteromer as a target. Furthermore, MCC22 was much more potent when administered intrathecally as compared to the brain [2], suggesting the spinal cord as a primary site of action for its analgesic effects.

We examined the antinociceptive effects of MCC22 in HbSS Townes mice and underlying mechanisms. MCC22 potently attenuated hyperalgesia without tolerance, decreased pro-inflammatory cytokines and increased the anti-inflammatory cytokine, IL-10, in the spinal cord, and decreased evoked responses of nociceptive dorsal horn neurons.

2. Methods

2.1. Animals

Adult, male Townes transgenic mice (4–12 weeks of age, 20–25g) which exclusively express human sickle hemoglobin (HbSS), human hemoglobin heterozygotes (HbAS), and normal human hemoglobin (HbAA controls) were used in this study. Genotypes were confirmed by polymerase chain reaction per the Jackson Laboratory protocol and high performance liquid chromatography [56]. Mice were housed four mice per cage, maintained on a 12-h light-dark cycle, and had access to food and water *ad libitum*. The three mouse strains, HbAA, HbAS and HbSS, were used to characterize mechanical hyperalgesia in all strains of Townes mice while only the more severe hyperalgesic HbSS mice and controls were used to evaluate drug effects. Mice were randomly selected to treatments and conditions. All procedures were approved by the University of Minnesota Institutional Animal Care and Use Committee.

2.2. Drugs and administration

All compounds were synthesized as described previously [2]. MCC22 consists of a mu opioid pharmacophore derived from the mu opioid agonist, oxymorphone, linked through a 22-atom spacer to the CCR5 antagonist pharmacophore, TAK220 (1-acetyl-N-[3-[4-[(4-carbamoylphenyl)methyl]piperidin-1-yl]propyl]-N-(3-chloro-4-methylphenyl)piperidine-4-carboxamide). MCC22 was initially dissolved in 10% dimethyl sulfoxide (DMSO) (Fisher Scientific, Hampton NH) and was diluted to less than 1% DMSO prior to administration. Homologs of MCC22 with spacer lengths of 14- and 24-atoms served as controls. Morphine (Mallinckrodt Inc., Hazlewood, MO) was dissolved in distilled water. All compounds were administered intraperitoneally (i.p.) to determine peak time and $ED_{50/80}$ values. Once determined, the ED_{80} doses were used for all experiments.

2.3. Behavioral measures of mechanical hyperalgesia

Cutaneous mechanical hyperalgesia was assessed as described previously [2,8,10,31]. The frequency of paw withdrawal evoked by a calibrated von Frey monofilament (North Coast Medical, Inc., Gilroy, CA) with a bending force 9.3 mN applied to the plantar surface of the hind paws for 1–2 seconds was deterrmined. Mice were placed beneath individual glass containers on a raised wire mesh surface and allowed to habituate for 15 min. The monofilament was applied to each hind paw 10 times at intervals of at least 3 seconds, and the average number of withdrawal responses was determined for each paw. Mechanical withdrawal threshold was determined using a pressure-meter [13] consisting of a hand-held force transducer fitted with a polypropylene tip (electronic von Frey anesthesiometer, IITC Inc., Life Science Instruments, Woodland Hills, CA, USA). The intensity of the stimulus was automatically recorded upon paw withdrawal. Withdrawal threshold was defined as the mean from three trials. The experimenter was blinded to the treatment condition.

Mechanical hyperalgesia in deep tissues was assessed by determining forepaw grip force measured using a computerized grip force meter (Chatillon Ametek, Largo, FL) as we described previously, [8,31] each mouse was held by its tail and gently passed over a wire mesh grid. The peak force was recorded in grams. Grip force was defined as the mean from three trials.

2.4. Electrophysiology

Electrophysiological recordings were made from nociceptive dorsal horn neurons as described previously [10]. Mice were anesthetized with 2.0% isoflurane (Kent Scientific, Torrington, CT) and given dexamethasone (5.0 mg/kg, s.c.) to prevent swelling and continuous saline (0.2 ml/hr sq) to maintain hydration. A feedback-controlled heating pad (Physitemp Instruments, Inc., Clifton, NJ) was used to maintain core body temperature at ~37°C using. Respiration rate and blood pressure were monitored continuously. Following depilation, an incision was made over the thoracic and lumbar regions of the vertebral column, a laminectomy exposed the lumbar enlargement at L4–L5, and mice were secured in a spinal frame. Isoflurane was reduced to 0.8–1.2% and a reservoir around the spinal column was made of vinyl polysiloxane dental impression material (3M ESPE Dental Products, St. Paul, MN) and filled with warm artificial cerebrospinal fluid. Following removal of the dura mater, extracellular recordings were made from dorsal horn neurons with receptive fields (RFs) located on the plantar surface of the hind paw using glass microelectrodes (~1 mΩ Kation Scientific, Minneapolis, MN) lowered into the spinal cord in 3-μm steps using an electric microdrive (Kopf, Tujunga, CA). Action potentials were amplified, audiomonitored, and displayed on a storage oscilloscope. Receptive fields of dorsal horn neurons were searched for by lightly stroking the skin and applying mild pressure with the experimenter's fingers. Neurons were functionally classified as low threshold (LT), wide dynamic range (WDR) or high threshold (HT) cells using mechanical stimulation of graded intensities (brushing, light and strong pressure using fine arterial clips, and pinch with forceps) as described previously [10]. Receptive field areas were mapped using suprathreshold von Frey monofilaments and drawn on a schematic of the hind paw. Only WDR neurons with action potentials easily discriminated by amplitude and shape were studied.

2.5. RNA isolation and real time PCR

Mice underwent cardiac perfusion with PBS, and spinal cords were removed (4 mice per group). RNA was isolated from whole spinal cords using Trizol and was DNAse treated (Invitrogen, Amsterdam) and was converted into cDNA using oligo(dT)$_{12–18}$ primers with the Advantage RT for PCR Kit (Takara). Real time PCR reactions were conducted with Rotor-Gene SYBR Green PCR kit (Qiagen). Briefly, 0.5μM primers, 1× SYBR Green Master Mix, and 2μl diluted cDNA were combined, and reactions were conducted in triplicates. The primers sequences have been previously published [46]. Real time PCR was conducted on a Qiagen Q real time PCR machine using a hot start with cycle conditions, 40 cycles; 95°C 15 seconds, 60°C 10 seconds, and 72°C 15 seconds; followed by a melt from 75°C to 95°C. Quantitation of the mRNA was based on standard curves derived from cDNA standards for each primer set from 1fg/μg of RNA to 100ng/μg of RNA. Positive and negative cDNA controls were used for each primer set derived from known cell sources for each cytokine. Samples were normalized to the expression of β-actin.

2.6. Experimental Design

Anti-hyperalgesia—In separate groups of mice, withdrawal response frequencies were determined prior to treatment and ED$_{50/80}$ doses were established for i.p. administration. For

each injection, withdrawal frequencies were determined at various times after injection to determine the duration of anti-hyperalgesia produced by each dose. In some experiments, MCC22 was given daily for up to 9 days to determine if MCC22 exhibited acute or chronic tolerance.

Tolerance—HbSS mice received two i.p. injections daily (one in the morning and one in the afternoon, 6 h apart) of MCC22 8.0 μmoles/kg (10 mg/kg) or morphine 26.4 μmoles/kg (10 mg/kg) for 9 consecutive days and withdrawal response frequencies were determined before injection, and on treatment days 1, 3 and 9, at 30 min after the second injection. Withdrawal response frequencies were determined before and at 30 min after MCC22.

Electrophysiology—Once a nociceptive neuron was identified, spontaneous and evoked responses were obtained before any injection, 30 minutes after i.p. administration of vehicle, and at 30 minutes after i.p. administration of MCC22. First, the discharge rate (impulses/s) of ongoing, spontaneous activity was determined for a period of 3 minutes. Next, mechanical response thresholds were determined using von Frey monofilaments. Threshold (mN) was defined as the weakest force to evoke a response that was clearly above any ongoing activity in at least 50% of the trials (8–10 trials). To obtain responses evoked by suprathreshold stimuli, an increasing series of von Frey monofilaments (1.0, 8.0, and 15.0 g; 9.3, 73.6 and 135.3 mN, respectively) were each applied three times for 5 s in ascending order. Each stimulus was applied to random locations within the RF with an inter-stimulus interval of at least 30 s. Next, heat (30–50° C) and cold (30–5° C) stimuli were applied to the RF using a Peltier-type thermode (5 mm^2). Beginning from a base temperature of 30° C, stimuli were delivered with a continuous ramp at a rate of 2.0° C/s and maintained for 1 s. Action potentials were discriminated using Spike II software (Cambridge Electronic Design, Cambridge, UK), and were stored on a computer along with the time of mechanical stimulation, and digitized traces of heat and cold stimul.

Cytokine expression—HbSS mice received twice daily injections of the ED_{80} dose of MCC22 or PBS (vehicle) for 9 consecutive days. The spinal cords were removed from HbSS mice administered MCC22 or PBS and from HbAA mice (4 mice per group). The RNA was isolated and converted to cDNA for use in real time PCR (triplicates) with primers for IL-1β, IL-6, IL-10, and TNFα. Samples were normalized based on expression of β-actin.

2.7. Data Analyses

Parametric statistics were used for all studies because data were normally distributed and displayed equal variance.

Behavior—Data are shown as mean (±SEM) values unless otherwise stated. Differences in withdrawal response thresholds, withdrawal response frequencies, and grip force between mouse strains were determined using one-way ANOVA. Drug effects on the magnitude and duration of anti-hyperalgesia, and tolerance, were compared between groups using one-way ANOVA. Post-hoc comparisons were made using Bonferroni *t*-tests. A probability value of $p<0.05$ was considered significant.

Electrophysiology—Comparisons were made in the responses of WDR neurons obtained in control, vehicle and drug conditions. Mechanical response thresholds were compared by one-way ANOVA. Discharge rates evoked by mechanical (von Frey) stimuli were determined by subtracting ongoing discharge rate during 10 s prior to the stimulus from the response that occurred during the stimulus (5 s) and for 5 s after. For each cell, mean responses evoked by each stimulus were obtained from three trials. Discharge rates evoked by each of the monofilaments for all neurons were compared between conditions using two-way ANOVA with repeated measures. Bonferroni *t*-tests were used for all post-hoc comparisons.

Cytokine expression—The expression of specific mRNA was determined using standard curves for each primer set. Samples were normalized based on β-actin expression. Significant differences between HbAA mice and between HbSS mice administered vehicle versus MCC22 was determined using one-way ANOVA with Bonferroni *t*-tests ($p<0.05$).

3. Results

3.1. Townes sickle mice exhibit robust mechanical hyperalgesia

As shown previously [37], HbSS Townes mice exhibited hyperalgesia indicated by a decrease in paw withdrawal threshold, an increase in paw withdrawal frequency, and a decrease in forelimb grip force as compared to HbAS and HbAA controls (Figure 1). HbSS mice had lower mechanical withdrawal thresholds compared to both HbAS and HbAA mice (Figure 1B; one-way ANOVA, $F(2, 105) = 59.39$, $p<0.001$), while withdrawal thresholds did not differ between HbAS and HbAA mice. Also, both HbSS and HbAS mice exhibited greater paw withdrawal frequencies than control HbAA mice, although withdrawal frequency in HbAS mice was less than that of HbAS mice (Figure 1A; one-way ANOVA, $F(2, 33) = 123.11$, $p<0.001$). Similarly, HbSS and HbAS mice had lower forelimb grip force compared to HbAA mice (Figure 1C; one-way ANOVA, $F(2, 51) = 31.13$, $p<0.001$), although this was more pronounced in HbSS mice ($p<0.001$).

3.2. MCC22 produces dose-dependent and long-lasting anti-hyperalgesia in sickle mice

We compared efficacies of MCC22 and morphine in HbSS mice. Both MCC22 and morphine reduced mechanical hyperalgesia dose-dependently. The ED_{50} for MCC22 was 0.88 μmol/kg, which was lower than that of morphine (5.84 μmol/kg; Figure 2A; one-way ANOVA, $F(6, 77) = 127.69$, $p<0.001$). MCC22 also produced a longer duration of anti-hyperalgesia than morphine (Figure 2B; one-way ANOVA with repeated measures, $F(5, 40) = 28.03$, $p<0.001$; and 2C; One-way ANOVA with repeated measures, $F(5, 25) = 14.29$, $p<0.001$). A reduction in paw withdrawal frequency produced by 8.0 μmol/kg (10 mg/kg) of MCC22 (ED_{80} dose) occurred 10 min after injection and peaked at 30 min. MCC22 produced a maximal reduction in paw withdrawal frequency of more than 90% in HbSS mice that persisted for at least 4 h after injection, at which time there was still approximately 30% inhibition of hyperalgesia. Paw withdrawal frequency returned to pre-injection values at 24 h. Anti-hyperalgesia following the ED_{80} dose for morphine (26.4 μmol/kg; 10 mg/kg) peaked at 30 min and produced a maximal reduction in paw withdrawal frequency of 73.0%. Following morphine, hyperalgesia recovered more quickly as compared to MCC22, and

there was a 41% inhibition of hyperalgesia 1 h after injection, as compared to 30% at 4 h after MCC22. Hyperalgesia recovered by 2 h after injection of morphine and did not differ from baseline.

3.3. MCC22 did not produce tolerance to its antihyperalgesic effect

It is well known that tolerance occurs with repeated administration of opioids resulting in the need for higher doses that limits their use. Therefore, we examined the extent to which tolerance occurred following repeated administration of MCC22 and compared this to morphine. We compared the anti-hyperalgesia produced by repeated administration of the ED_{80} dose for MCC22 (8.0 μmol/kg) to that produced by repeated administration of the ED_{80} dose for morphine (26.4 μmol/kg) in separate groups of HbSS mice. Mice were given twice daily injections of either MCC22 or morphine for 9 consecutive days. Withdrawal response frequencies were determined before and at 30 min after injection of MCC22 (Figure 3A) or morphine (Figure 3B) on day 1, 3 and 9 of treatment. Tolerance was not observed following MCC22 and consistently produced maximal anti-hyperalgesia over the 9-day time-course (one-way ANOVA with repeated measures, $F(5, 39) = 237.43$, $p<0.001$). Unexpectedly, during this period baseline withdrawal response frequencies gradually decreased in MCC22-treated mice. In contrast, morphine exhibited tolerance as early as day 3 (one-way ANOVA with repeated measures, $F(5, 38) = 38.84$, $p<0.001$) and did not produce any anti-hyperalgesia by day 9 of treatment. These results show that unlike morphine, MCC22 does not produce tolerance to its antihyperalgesic properties over the 9-day time course.

3.4. Evoked responses of dorsal horn neurons in sickle mice were reduced by MCC22

Eight mechanosensitive WDR neurons were studied from 8 HbSS mice. Recording sites were in the dorsal horn at depths from 243 to 588 μm below the surface of the spinal cord. Receptive fields were located on the plantar surface of the hind paw. None of the neurons were spontaneously active, and two were responsive to heat stimuli and two were excited by cold stimuli. Evoked responses were obtained before any drug injection, at 30 min after vehicle injection, and at 30 min following MCC22 (8 μmol/kg). MCC22, but not vehicle, dramatically decreased evoked responses to mechanical and thermal stimuli. Figure 4A shows mean discharge rates (impulses/s) evoked by 8.0 and 15.0 g von Frey monofilaments before any injection, after vehicle, and after MCC22. MCC22, but not vehicle, dramatically reduced mean discharge rates evoked by stimuli of 1.0, 8.0, and 15.0 g (Figure 4A; (two-way ANOVA with repeated measures, $F(2, 63) = 46.81$, $p<0.001$). Discharge rates evoked by 8.0 and 15.0 g decreased from16.5 ±2.9 and 46.2 ±5.8 impulses/s, respectively, before MCC22 (after injection of vehicle) to 1.2 ±0.5 and 2.3 ±0.8 impulses/s, respectively, after MCC22 Discharge rates evoked by 1.0 g decreased from 2.5 ±0.6 to 0.6 ±0.2, but this was not statistically significant. There was a significant interaction between treatment and von Frey stimulus intensity (two-way ANOVA with repeated measures, $F(4, 63) = 17.29$, $p<0.001$). As seen in figure 4, the extent to which MCC22 decreases mean discharge rates is significantly greater with increasing levels of von Frey filaments. MCC22 also increased mean response thresholds for all neurons (One-way ANOVA, $F(2, 21) = 10.33$, $p<0.001$). Mean response thresholds did not change after injection of vehicle (4.7 ±0.44 mN before and 5.0 ±0.43 mN after) but increased to 7.9 ±0.74 mN after injection of MCC22

(Bonferroni t-test, $p<0.004$). A representative example of the functional characterization (Figure 4B) and mechanically-evoked responses before and after injection of vehicle and MCC22 for a single WDR neuron is illustrated in Figure 4C–E.

Four of the eight WDR neurons studied were also responsive to noxious cold (5° C; n=2) and to noxious heat (50° C; n=2). Responses of individual WDR neurons to cold and heat are illustrated in Figure 5A and 5B, respectively, and were not altered following administration of vehicle but were greatly reduced following MCC22.

3.5. MCC22 reduces pro-inflammatory cytokines and increases anti-inflammatory cytokines the spinal cord

Pro-inflammatory cytokines released by activated microglia contributes to sensitization of nociceptive neurons in the spinal cord. Pro-inflammatory cytokines have been associated with chronic pain, including neuropathic pain. We determined whether MCC22 decreased pro-inflammatory cytokines and/or increased anti-inflammatory cytokines as a possible mechanism for its antihyperalgesic effect. HbSS mice with mechanical hyperalgesia that were treated twice daily for 9 days with vehicle had increased expression of the pro-inflammatory cytokines, IL-1β, IL-6, and TNFα, in the spinal cord as compared to HbAA mice (Figure 6). One-Way ANOVAs showed that the expression of these cytokines was decreased significantly in HbSS mice given MCC22 (8 μmol/kg) twice daily for 9 consecutive days (IL-1β; $F(2, 6) = 1310.0$, $p<0.0001$; IL-6; $F(2, 6) = 1273.0$, $p<0.0001$; TNFα; $F(2, 6) = 1376.0$, $p<0.0001$). Thus, microglia are a possible target for MCC22 since they express both MOR and CCR5.

Figure 6 shows that expression of the anti-inflammatory cytokine, IL-10, in the spinal cord was increased following MCC22 as compared to HbAA mice and HbSS mice treated with vehicle for 9 days (One-way ANOVA, $F(2, 6) = 754.1$, $p<0.0001$). IL-10 has been shown to decrease hyperalgesia in inflammatory and neuropathic pain models [35,43,52,76]. Thus, the increase in IL-10 may contribute to the analgesic efficacy of MCC22.

4. Discussion

Targeting multiple receptors with multifunctional or bivalent ligands may be an effective approach for treating pain. Ligands that target opioid/NK-1 [59], opioid/nociceptin [60], opioid/CB1 [33,44], opioid/metabotropic glutamate receptor-5 [57] and multiple opioid receptors [1,34,53] were found to be effective analgesics having enhanced potency in pre-clinical models. MCC22 differs from previous ligands in that it targets mu opioid and a chemokine receptor, CCR5. This makes MCC22 unique because it targets CCR5 (and MOR) on glial cells to inhibit glial activation and pro-inflammatory cytokines that contribute to central sensitization, and MOR located on neurons (and perhaps glia) to decrease neuronal excitability. Although direct binding studies have not been done, molecular modeling and simulation studies suggest that MCC22 is capable of binding to both MOR and CCR5 [2]. The combined action of MCC22 on glial cells and neurons may account for its extraordinary potency.

Opioids are a primary treatment for chronic, severe pain in patients with SCD. Given the many undesirable side effects associated with opioids, new approaches for managing severe chronic pain are needed. The results of this study show that the novel bivalent ligand, MCC22, which targets mu opioid receptors and CCR5, produced dose-dependent, potent anti-hyperalgesia in a transgenic mouse model of SCD. Importantly, MCC22 did not produce analgesic tolerance, at least over a 9-day period when given twice per day whereas administration of morphine given over the same time course resulted in substantial tolerance.

Psychophysical studies using quantitative sensory testing have shown that SCD patients have greater sensitivity to mechanical, heat and cold stimuli [7] that is likely due to both peripheral and central mechanisms. For example, in the periphery, sickle mice exhibited increases in immunoreactivity for substance P and calcitonin gene-related peptide (neuropeptides found in nociceptive neurons), neurogenic inflammation, activation of mast cells, nerve sprouting, decreased innervation (indicative of neuropathy), and sensitization of nociceptors [27,31,66,69]. In the spinal cord, sickle mice had elevated phosphorylated MAP kinases, activated astrocytes and microglia, and up-regulation of TLR4, IL-6, STAT3 and COX-2 [31,68]. These changes, as well as increases in pro-inflammatory cytokines IL-1β, IL-6, and TNFα found in the present study likely contribute to the increased responses of dorsal horn neurons (central sensitization) described in sickle mice [10]. Similarly, patients with SCD also had elevated plasma levels of cytokines that include IL-1β, IL-6, and TNFα, and substance P [9,54], and psychophysical studies of pain tolerance and central summation of evoked pain suggested that pain in SCD is associated with central sensitization [9]. In addition to inflammatory pain, neuropathic pain has been described in sickle mice as evidenced by decreased cutaneous innervation [31], and nearly 40% of patients had evidence of neuropathic pain based on sensory symptoms [6].

The anti-hyperalgesia produced by MCC22 in the present study was concomitant with a decrease in the expression of pro-inflammatory cytokines in the spinal cord and decreased evoked responses nociceptive dorsal horn neurons. Interactions between glia and neurons contribute to hyperalgesia through the release of pro-inflammatory cytokines from glial cells that sensitize proximal dorsal horn neurons [21,65,75]. It is possible that MCC22 blocks this process by reducing the release of the pro-inflammatory cytokines IL-1β, IL-6 and TNFα, which contribute to central sensitization [3,30]. Interestingly, MCC22 also increased the expression of the anti-inflammatory cytokine, IL-10, which might represent a compensatory mechanism associated with the increase in the pro-inflammatory cytokines produced by the disease, or be a direct effect of MCC22. Indeed, targeting specific inflammatory pathways is a general therapeutic approach for SCD [47].

The specific 22-atom linker requirement for the extraordinary potency of MCC22-produced anti-hyperalgesia and the results of molecular simulation studies have suggested the targeting of a MOR-CCR5 heteromer [2]. The spacer length was based on prior studies that suggested effective bridging of heteromeric GPCR protomers in the range of 18–22 atoms [77] and on molecular simulation studies of the interaction of MCC22 with a MOR-CCR5 heteromer that were consistent with bridging of MOR and CCR5 protomers [2].

The ability for G protein-coupled receptors (GPCRs) to form heteromers has been established [17,22]. Receptor heterodimerization can alter receptor function, ligand pharmacology, signal transduction, and cellular trafficking [26]. Thus, targeting GPCR heteromers may result in more potent compounds that selective act on cells that co-express both receptors [28].

With respect to opioid receptors, it has been shown that they can form heteromers with a number of different GPCRs and that the propensity for MORs to form dimers with other GPCRs may be modulated in pathological states [20]. It is known that MOR interacts with other GPCRs through the formation of heteromers [20]. For example, mu-delta (MOR-DOR) opioid receptor heteromers have been identified and ligands targeting this heteromer produced potent analgesia [1,74]. MMG22, another bivalent ligand consisting of mu opioid agonist and metabotrophic glutamate receptor 5 antagonist pharmacophores, displayed exceptionally potent antinociception following intrathecal administration in mouse models of acute inflammatory pain and cancer pain without the side effects associated with clinically employed opioids [57].

Importantly, there is evidence that MOR-CCR5 heteromers may exist *in vivo*. Both receptors are present in neurons and glia in the dorsal horn, and are co-localized in other areas of pain processing [25,36]. Thus, functional interactions between MOR and CCR5 receptors located on glia and/or neurons may contribute to chronic pain, perhaps by desensitization of MOR upon activation of CCR5 [62]. Since pro-inflammatory cytokines from activated microglia in the spinal cord contribute to hyperalgesia via central sensitization, targeting a MOR-CCR5 heteromer with concomitant activation of MOR and blockade of CCR5 was considered as an approach to inhibiting activated microglia for developing effective analgesics for chronic pain [2]. Significantly, MCC22 given daily for 9 days reduced the enhanced expression of pro-inflammatory cytokines in the spinal cord of sickle mice. It is unknown from the present studies whether the decrease in cytokines following MCC22 contributed to the decrease in responses of dorsal horn neurons. Also, it is not known whether a decrease in pro-inflammatory cytokines contributes to the decrease in hyperalgesia and responses of dorsal horn neurons following a single injection of MCC22 or whether these changes occur through a different mechanism. However, a cytokine-related mechanism is a possibility since there is ongoing inflammation in sickle mice and in patients. It is unclear how MCC22 produced a profound decrease in pro-inflammatory cytokines, but previous studies showing that chronic intrathecal administration of a CCR5 antagonist decreased neuropathic pain, also reported a decrease in pro-inflammatory and an increase in anti-inflammatory cytokines in the spinal cord [50]. Indeed, antinociception produced by MCC22 was blocked by the microglia inhibitor, minocycline [2], suggesting that MCC22 might interact with activated glial cells and thereby reduce excitability of dorsal horn neurons. Further studies are needed to elucidate specific effects of MCC22 on glial cells and their neuronal interactions.

A common side effect of clinically employed opioids is tolerance which leads to the need for elevated doses to achieve the desired effect [15]. Remarkably, tolerance was not observed following repeated daily administration of MCC22, and baseline paw withdrawal frequencies unexpectedly decreased over time. While it is unclear why baseline withdrawal responses decreased over time following repeated administration of MCC22, this may be

related to the pharmacokinetic excretion of MCC22 or modulation of the MOR-CCR5 heteromer with repeated activation. Intrinsic receptor mechanisms such as receptor internalization and desensitization contribute to opioid tolerance [73] and it is unknown whether MCC22 alters the kinetics and receptor trafficking that lead to down-regulation or desensitization of MOR. In this regard, it was reported that blockade of microglia reduced opioid tolerance and increased analgesic efficacy [71].

In conclusion, our studies indicate that MCC22 produced potent antinociception in sickle mice and decreased responses of nociceptive dorsal horn neurons. These changes were associated with decreased levels of pro-inflammatory cytokines (IL-1β, IL-6, TNFα) and increased levels of the anti-inflammatory cytokine, IL-10 in the spinal cord. The finding that MCC22 was highly effective in inhibiting hyperalgesia without producing tolerance in hyperalgesic sickle mice suggests potential use for treatment of other painful inflammatory and neuropathic disorders. Strategic targeting of heteromers may be an effective alternative to traditional opioids for the treatment of chronic pain conditions.

Acknowledgments

This work was supported by the National Heart, Lung, and Blood Institute grants R01 HL135895 (DAS), R01 HL114567-05 (GMV and JDB), and R01 DA030316 (PSP).

References

1. Aceto MD, Harris LS, Negus SS, Banks ML, Hughes LD, Akgün E, Portoghese PS. MDAN-21: A bivalent opioid ligand containing mu-agonist and delta-antagonist pharmacophores and its effects in Rhesus Monkeys. Int J Med Chem. 2012; 2012:327257. [PubMed: 25954526]
2. Akgün E, Javed MI, Lunzer MM, Powers MD, Sham YY, Watanabe Y, Portoghese PS. Inhibition of Inflammatory and Neuropathic Pain by Targeting a Mu Opioid Receptor/Chemokine Receptor5 Heteromer (MOR-CCR5). Journal of Medicinal Chemistry. 2015; 58(21):8647–8657. [PubMed: 26451468]
3. Andrade P, Visser-Vandewalle V, Hoffmann C, Steinbusch HWM, Daemen MA, Hoogland G. Role of TNF-alpha during central sensitization in preclinical studies. Neurol Sci. 2011; 32:757–771. [PubMed: 21559854]
4. Ballas SK, Gupta K, Adams-Graves P. Sickle cell pain: a critical reappraisal. Blood. 2012; 120(18): 3647–3656. [PubMed: 22923496]
5. Belcher JD, Bryant CJ, Nguyen J, Bowlin PR, Kielbik MC, Bischof JC, Hebbel RP, Vercellotti GM. Transgenic sickle mice have vascular inflammation. Blood. 2003; 101(10):3953–3959. [PubMed: 12543857]
6. Brandow A, Farley R, Panepinto J. Neuropathic Pain in Patients with Sickle Cell Disease. Pediatr Blood Cancer. 2014; 61(3):512–517. [PubMed: 24167104]
7. Brandow AM, Stucky CL, Hillery CA, Hoffmann RG, Panepinto JA. Patients with sickle cell disease have increased sensitivity to cold and heat. Am J Hematol. 2013; 88(1):37–43. [PubMed: 23115062]
8. Cain DM, Vang D, Simone DA, Hebbel RP, Gupta K. Mouse models for studying pain in sickle disease: effects of strain, age, and acuteness. Br J Haematol. 2012; 156(4):535–544. [PubMed: 22171826]
9. Campbell CM, Carroll CP, Kiley K, Han D, Haywood C Jr, Lanzkron S, Swedberg L, Edwards RR, Page GG, Haythornthwaite JA. Quantitative sensory testing and pain-evoked cytokine reactivity: comparison of patients with sickle cell disease to healthy matched controls. Pain. 2016; 157(4):949–956. [PubMed: 26713424]

10. Cataldo G, Rajput S, Gupta K, Simone DA. Sensitization of nociceptive spinal neurons contributes to pain in a transgenic model of sickle cell disease. Pain. 2015; 156(4):722–730. [PubMed: 25630029]
11. Chen C, Li J, Bot G, Szabo I, Rogers TJ, Liu-Chen L-Y. Heterodimerization and cross-desensitization between the μ-opioid receptor and the chemokine CCR5 receptor. European Journal of Pharmacology. 2004; 483(2–3):175–186. [PubMed: 14729105]
12. Clark AK, Gruber-Schoffnegger D, Drdla-Schutting R, Gerhold KJ, Malcangio M, Sandkuehler J. Selective activation of microglia facilitates synaptic strength. Journal of Neuroscience. 2015; 35:4552–4570. [PubMed: 25788673]
13. Cunha TM, Verri WA Jr, Vivancos GG, Moreira IF, Reis S, Parada CA, Cunha FQ, Ferreira SH. An electronic pressure-meter nociception paw test for mice. Braz J Med Biol Res. 2004; 37(3):401–407. [PubMed: 15060710]
14. Darbari D, Ballas S, Clauw D. Thinking beyond sickling to better understand pain in sickle cell disease. Eur J Haematol. 2014; 93:89–95. [PubMed: 24735098]
15. Dumas EO, Pollack GM. Opioid tolerance development: a pharmacokinetic/pharmacodynamic perspective. AAPS J. 2008; 10(4):537–551. [PubMed: 18989788]
16. El-Hage N, Wu G, Wang J, Ambati J, Knapp PE, Reed JL, Bruce-Keller AJ, Hauser KF. HIV-1 Tat and opiate-induced changes in astrocytes promote chemotaxis of microglia through the expression of MCP-1 and alternative chemokines. Glia. 2006; 53:132–146. [PubMed: 16206161]
17. Ferre S, Casado V, Devi LA, Filizola M, Jockers R, Lohse MJ, Milligan G, Pin JP, Guitart X. G protein-coupled receptor oligomerization revisited: functional and pharmacological perspectives. Pharmacol Rev. 2014; 66(2):413–434. [PubMed: 24515647]
18. Frenette P, Atweh G. Sickle cell disease: old discoveries, new concepts, and future promise. J Clin Invest. 2007; 117(4):850–858. [PubMed: 17404610]
19. Gao YJ, Ji RR. Chemokines, neuronal-glial interactions, and central processing of neuropathic pain. Pharmacol Ther. 2010; 126(1):56–68. [PubMed: 20117131]
20. Gomes I, Fujita W, Chandrakala MV, Devi LA. Disease-specific heteromerization of G-protein-coupled receptors that target drugs of abuse. Prog Mol Biol Transl Sci. 2013; 117:207–265. [PubMed: 23663971]
21. Grace PM, Hutchinson MR, Maier SF, Watkins LR. Pathological pain and the neuroimmune interface. Nat Rev Immunol. 2014; 14(4):217–231. [PubMed: 24577438]
22. Gurevich VV, Gurevich EV. How and why do GPCRs dimerize? Trends Pharmacol Sci. 2008; 29(5):234–240. [PubMed: 18384890]
23. Hang LH, Li SN, Dan X, Shu WW, Luo H, Shao DH. Involvement of Spinal CCR5/PKCgamma Signaling Pathway in the Maintenance of Cancer-Induced Bone Pain. Neurochem Res. 2017; 42(2):563–571. [PubMed: 27848062]
24. Hang LH, Shao DH, Chen Z, Chen YF, Shu WW, Zhao ZG. Involvement of spinal CC chemokine ligand 5 in the development of bone cancer pain in rats. Basic Clin Pharmacol Toxicol. 2013; 113(5):325–328. [PubMed: 23773283]
25. Happel C, Steele AD, Finley MJ, Kutzler MA, Rogers TJ. DAMGO-induced expression of chemokines and chemokine receptors: the role of TGF-β1. J Leukocyte Biol. 2008; 83:956–963. [PubMed: 18252865]
26. Hiller C, Kuhhorn J, Gmeiner P. Class A G-protein-coupled receptor (GPCR) dimers and bivalent ligands. J Med Chem. 2013; 56(17):6542–6559. [PubMed: 23678887]
27. Hillery CA, Kerstein PC, Vilceanu D, Barabas ME, Retherford D, Brandow AM, Wandersee NJ, Stucky CL. Transient receptor potential vanilloid 1 mediates pain in mice with severe sickle cell disease. Blood. 2011; 118(12):3376–3383. [PubMed: 21708890]
28. Hubner H, Schellhorn T, Gienger M, Schaab C, Kaindl J, Leeb L, Clark T, Moller D, Gmeiner P. Structure-guided development of heterodimer-selective GPCR ligands. Nat Commun. 2016; 7:12298. [PubMed: 27457610]
29. Kato G. New insights into sickle cell disease: mechanisms and investigational therapies. Curr Opin Hematol. 2016; 23(3):224–232. [PubMed: 27055046]
30. Kawasaki Y, Zhang L, Cheng J-K, Ji R-R. Cytokine mechanisms of central sensitization: distinct and overlapping role of interleukin-1β, interleukin-6, and tumor necrosis factor-α in regulating

synaptic and neuronal activity in the superficial spinal cord. J Neurosci. 2008; 28:5189–5194. [PubMed: 18480275]

31. Kohli DR, Li Y, Khasabov SG, Gupta P, Kehl LJ, Ericson ME, Nguyen J, Gupta V, Hebbel RP, Simone DA, Gupta K. Pain-related behaviors and neurochemical alterations in mice expressing sickle hemoglobin: modulation by cannabinoids. Blood. 2010; 116(3):456–465. [PubMed: 20304807]
32. Latremoliere A, Woolf CJ. Central sensitization: a generator of pain hypersensitivity by central neural plasticity. J Pain. 2009; 10:895–926. [PubMed: 19712899]
33. Le Naour M, Akgun E, Yekkirala A, Lunzer MM, Powers MD, Kalyuzhny AE, Portoghese PS. Bivalent ligands that target mu opioid (MOP) and cannabinoid1 (CB1) receptors are potent analgesics devoid of tolerance. J Med Chem. 2013; 56(13):5505–5513. [PubMed: 23734559]
34. Le Naour M, Lunzer MM, Powers MD, Kalyuzhny AE, Benneyworth MA, Thomas MJ, Portoghese PS. Putative kappa opioid heteromers as targets for developing analgesics free of adverse effects. J Med Chem. 2014; 57(15):6383–6392. [PubMed: 24978316]
35. Ledeboer A, Jekich BM, Sloane EM, Mahoney JH, Langer SJ, Milligan ED, Martin D, Maier SF, Johnson KW, Leinwand LA, Chavez RA, Watkins LR. Intrathecal interleukin-10 gene therapy attenuates paclitaxel-induced mechanical allodynia and proinflammatory cytokine expression in dorsal root ganglia in rats. Brain Behav Immun. 2007; 21(5):686–698. [PubMed: 17174526]
36. Lee YK, Choi D-Y, Jung Y-Y, Yun YW, Lee BJ, Han SB, Hong JT. Decreased pain responses of C-C chemokine receptor 5 knockout mice to chemical or inflammatory stimuli. Neuropharmacology. 2013; 67:57–65. [PubMed: 23147416]
37. Lei J, Benson B, Tran H, Ofori-Acquah SF, Gupta K. Comparative analysis of pain behaviours in humanized mouse models of sickle cell anemia. PLoS One. 2016; 11(8):e0160608. [PubMed: 27494522]
38. Liou JT, Lee CM, Day YJ. The immune aspect in neuropathic pain: role of chemokines. Acta Anaesthesiol Taiwan. 2013; 51(3):127–132. [PubMed: 24148742]
39. Liou JT, Mao CC, Ching-Wah Sum D, Liu FC, Lai YS, Li JC, Day YJ. Peritoneal administration of Met-RANTES attenuates inflammatory and nociceptive responses in a murine neuropathic pain model. J Pain. 2013; 14(1):24–35. [PubMed: 23183003]
40. Mahajan SD, Schwartz SA, Shanahan TC, Chawda RP, Nair MPN. Morphine regulates gene expression of α- and β-chemokines and their receptors on astroglial cells via the opioid μ receptor. J Immunology. 2002; 169:3589–3599. [PubMed: 12244149]
41. Matsushita K, Tozaki-Saitoh H, Kojima C, Masuda T, Tsuda M, Inoue K, Hoka S. Chemokine (C-C motif) receptor 5 is an important pathological regulator in the development and maintenance of neuropathic pain. Anesthesiology. 2014; 120:1491–1503. [PubMed: 24589480]
42. Mika J, Zychowska M, Popiolek-Barczyk K, Rojewska E, Przewlocka B. Importance of glial activation in neuropathic pain. Eur J Pharmacol. 2013; 716(1–3):106–119. [PubMed: 23500198]
43. Milligan ED, Sloane EM, Langer SJ, Cruz PE, Chacur M, Spataro L, Wieseler-Frank J, Hammack SE, Maier SF, Flotte TR, Forsayeth JR, Leinwand LA, Chavez R, Watkins LR. Controlling neuropathic pain by adeno-associated virus driven production of the anti-inflammatory cytokine, interleukin-10. Mol Pain. 2005; 1:9. [PubMed: 15813997]
44. Mollica A, Pelliccia S, Famiglini V, Stefanucci A, Macedonio G, Chiavaroli A, Orlando G, Brunetti L, Ferrante C, Pieretti S, Novellino E, Benyhe S, Zador F, Erdei A, Szucs E, Samavati R, Dvrorasko S, Tomboly C, Ragno R, Patsilinakos A, Silvestri R. Exploring the first Rimonabant analog-opioid peptide hybrid compound, as bivalent ligand for CB1 and opioid receptors. J Enzyme Inhib Med Chem. 2017; 32(1):444–451. [PubMed: 28097916]
45. Nur E, Biemond BJ, Otten HM, Brandjes DP, Schnog JJ, Group CS. Oxidative stress in sickle cell disease; pathophysiology and potential implications for disease management. Am J Hematol. 2011; 86(6):484–489. [PubMed: 21544855]
46. Olson J, Miller S. Microglia initiate central nervous system innate and adaptive immune responses through multiple TLRs. J Immunol. 2004; 173:3916–3924. [PubMed: 15356140]
47. Owusu-Ansah A, Ihunnah CA, Walker AL, Ofori-Acquah SF. Inflammatory targets of therapy in sickle cell disease. Transl Res. 2016; 167(1):281–297. [PubMed: 26226206]

48. Parsadaniantz SM, Rivat C, Rostene W, Goazigo AR-L. Opioid and chemokine receptor crosstalk: a promising target for pain therapy. Nat Rev Neurosci. 2015; 16:69–78. [PubMed: 25588373]
49. Piel FB, Steinberg MH, Rees DC. Sickle Cell Disease. N Engl J Med. 2017; 376(16):1561–1573. [PubMed: 28423290]
50. Piotrowska A, Kwiatkowski K, Rojewska E, Makuch W, Mika J. Maraviroc reduces neuropathic pain through polarization of microglia and astroglia - Evidence from in vivo and in vitro studies. Neuropharmacology. 2016; 108:207–219. [PubMed: 27117708]
51. Platt OS, Thorington BD, Brambilla DJ, Milner PF, Rosse WF, Vichinsky E, Kinney TR. Pain in sickle cell disease. Rates and risk factors. N Engl J Med. 1991; 325(1):11–16. [PubMed: 1710777]
52. Poole S, Cunha FQ, Selkirk S, Lorenzetti BB, Ferreira SH. Cytokine-mediated inflammatory hyperalgesia limited by interleukin-10. Br J Pharmacol. 1995; 115(4):684–688. [PubMed: 7582491]
53. Prezzavento O, Arena E, Sanchez-Fernandez C, Turnaturi R, Parenti C, Marrazzo A, Catalano R, Amata E, Pasquinucci L, Cobos EJ. (+)-and (−)-Phenazocine enantiomers: Evaluation of their dual opioid agonist/sigma1 antagonist properties and antinociceptive effects. Eur J Med Chem. 2017; 125:603–610. [PubMed: 27721146]
54. Qari MH, Dier U, Mousa SA. Biomarkers of inflammation, growth factor, and coagulation activation in patients with sickle cell disease. Clin Appl Thromb Hemost. 2012; 18(2):195–200. [PubMed: 21949038]
55. Ramesh G, MacLean AG, Philipp MT. Cytokines and chemokines at the crossroads of neuroinflammation, neurodegeneration, and neuropathic pain. Mediators Inflamm. 2013; 2013:480739. [PubMed: 23997430]
56. Shi PA, Choi E, Chintagari NR, Nguyen J, Guo X, Yazdanbakhsh K, Mohandas N, Alayash AI, Manci EA, Belcher JD, Vercellotti GM. Sustained treatment of sickle cell mice with haptoglobin increases HO-1 and H-ferritin expression and decreases iron deposition in the kidney without improvement in kidney function. Br J Haematol. 2016; 175(4):714–723. [PubMed: 27507623]
57. Smeester BA, Lunzer MM, Akgun E, Beitz AJ, Portoghese PS. Targeting putative mu opioid/metabotropic glutamate receptor-5 heteromers produces potent antinociception in a chronic murine bone cancer model. Eur J Pharmacol. 2014; 743:48–52. [PubMed: 25239072]
58. Song C, Rahim RT, Davey PC, Bednar F, Bardi G, Zhang L, Zhang N, Oppenheim JJ, Rogers TJ. Protein kinase Cζ mediates μ-opioid receptor-induced cross-desensitization of chemokine receptor CCR5. J Biol Chem. 2011; 286(23):20354–20365. [PubMed: 21454526]
59. Starnowska J, Costante R, Guillemyn K, Popiolek-Barczyk K, Chung NN, Lemieux C, Keresztes A, Van Duppen J, Mollica A, Streicher J, Vanden Broeck J, Schiller PW, Tourwe D, Mika J, Ballet S, Przewlocka B. Analgesic properties of opioid/NK1 multitarget ligands with distinct in vitro profiles in naive and chronic constriction injury mice. ACS Chem Neurosci. 2017; 8(10):2315–2324. [PubMed: 28699350]
60. Starnowska J, Guillemyn K, Makuch W, Mika J, Ballet S, Przewlocka B. Bifunctional opioid/nociceptin hybrid KGNOP1 effectively attenuates pain-related behaviour in a rat model of neuropathy. Eur J Pharm Sci. 2017; 104:221–229. [PubMed: 28347772]
61. Suzuki S, Chuang LF, Yau P, Doi RH, Chuang RY. Interactions of opioid and chemokine receptors: Oligomerization of mu, kappa, and delta with CCR5 on immune cells. Exp Cell Res. 2002; 280(2): 192–200. [PubMed: 12413885]
62. Szabo I, Chen XH, Xin L, Adler MW, Howard OM, Oppenheim JJ, Rogers TJ. Heterologous desensitization of opioid receptors by chemokines inhibits chemotaxis and enhances the perception of pain. Proc Natl Acad Sci U S A. 2002; 99(16):10276–10281. [PubMed: 12130663]
63. Szabo I, Wetzel MA, Zhang N, Steele AD, Kaminsky DE, Chen C, Liu-Chen L-Y, Bednar F, Henderson EE, Howard OMZ, Oppenheim JJ, Rogers TJ. Selective inactivation of CCR5 and decreased infectivity of R5 HIV-1 strains mediated by opioid-induced heterologous desensitization. J Leukoc Biol. 2003; 74(6):1074–1082. [PubMed: 12972507]
64. Takashima K, Miyake H, Kanzaki N, Tagawa Y, Wang X, Sugihara Y, Iizawa Y, Baba M. Highly potent inhibition of human immunodeficiency virus type 1 replication by TAK-220, an orally bioavailable small-molecule CCR5 antagonist. Antimicrob Agents and Chemother. 2005; 49(8): 3474–3482. [PubMed: 16048963]

65. Tsuda M. Modulation of Pain and Itch by Spinal Glia. Neurosci Bull. 2017
66. Uhelski ML, Gupta K, Simone DA. Sensitization of C-fiber nociceptors in mice with sickle cell disease is decreased by local inhibition of anandamide hydrolysis. Pain. 2017; 158(9):1711–1722. [PubMed: 28570479]
67. Vallejo R, Tilley DM, Vogel L, Benyamin R. The role of glia and the immune system in the development and maintenance of neuropathic pain. Pain Pract. 2010; 10(3):167–184. [PubMed: 20384965]
68. Valverde Y, Benson B, Gupta M, Gupta K. Spinal glial activation and oxidative stress are alleviated by treatment with curcumin or coenzyme Q in sickle mice. Haematologica. 2016; 101(2):e44–47. [PubMed: 26546503]
69. Vincent L, Vang D, Nguyen J, Gupta M, Luk K, Ericson ME, Simone DA, Gupta K. Mast cell activation contributes to sickle cell pathobiology and pain in mice. Blood. 2013; 122(11):1853–1862. [PubMed: 23775718]
70. Watkins LR, Hutchinson MR, Johnston IN, Maier SF. Glia: novel counter-regulators of opioid analgesia. Trends in Neurosci. 2005; 28(12):661–669.
71. Watkins LR, Hutchinson MR, Rice KC, Maier SF. The “Toll” of Opioid-Induced Glial Activation: Improving the Clinical Efficacy of Opioids by Targeting Glia. Trends Pharmacol Sci. 2009; 30(11):581–591. [PubMed: 19762094]
72. Weiss U. Derivatives of morphine. I. 14-Hydroxydihydromorphinone. J Am Chem Soc. 1955; 77(22):5891–5892.
73. Williams JT, Ingram SL, Henderson G, Chavkin C, von Zastrow M, Schulz S, Koch T, Evans CJ, Christie MJ. Regulation of μ-opioid receptors: desensitization, phosphorylation, internalization and tolerance. Pharmacol Rev. 2013; 65(1):223–254. [PubMed: 23321159]
74. Yekkirala AS, Banks ML, Lunzer MM, Negus SS, Rice KC, Portoghese PS. Clinically Employed Opioid Analgesics Produce Antinociception via μ-δ Opioid Receptor Heteromers in Rhesus Monkeys. ACS Chem Neurosci. 2012; 3:720–727. [PubMed: 23019498]
75. Zhang ZJ, Jiang BC, Gao YJ. Chemokines in neuron-glial cell interaction and pathogenesis of neuropathic pain. Cell Mol Life Sci. 2017; 74(18):3275–3291. [PubMed: 28389721]
76. Zheng W, Huang W, Liu S, Levitt RC, Candiotti KA, Lubarsky DA, Hao S. IL-10 mediated by herpes simplex virus vector reduces neuropathic pain induced by HIV gp120 combined with ddC in rats. Mol Pain. 2014; 10:49. [PubMed: 25078297]
77. Zheng Y, Akgün E, Harikumar KG, Hopson J, Powers MD, Lunzer MM, Miller LJ, Portoghese PS. Induced association of μ opioid (MOP) and type 2 cholecystokinin (CCK2) receptors by novel bivalent ligands. J Med Chem. 2009; 52:247–258. [PubMed: 19113864]
78. Zhuo M, Wu G, Wu LJ. Neuronal and microglial mechanisms of neuropathic pain. Mol Brain. 2011; 4:31. [PubMed: 21801430]

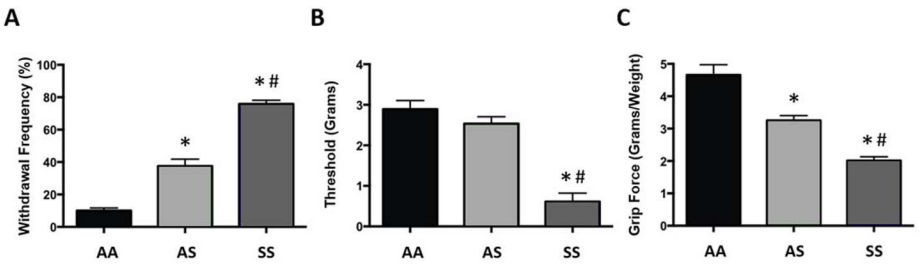

Figure 1.

Characterization of mechanical hyperalgesia in Townes mice. **(A)** Mean paw withdrawal frequency (n=12), **(B)** mean paw withdrawal threshold (n=36), and **(C)** mean forelimb grip (n=18) in Townes AA, AS and SS mice. * indicates a significant difference from AA mice; Bonferroni t-test; $p<0.001$; # indicates a significant difference from AS mice; Bonferroni t-test; $p<0.001$.

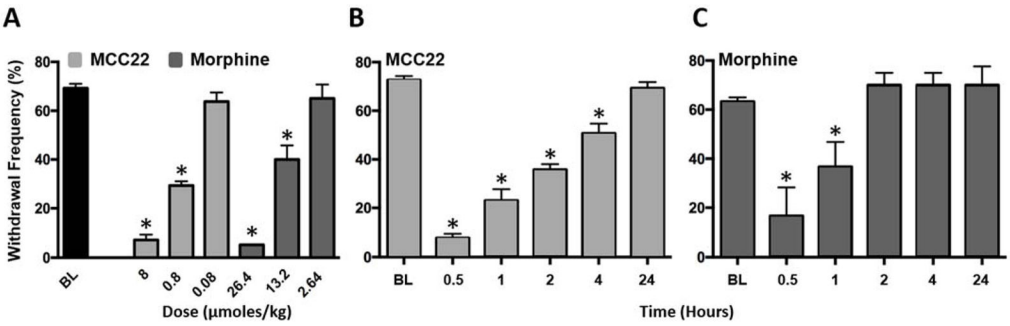

Figure 2.

Magnitude and duration of anti-hyperalgesia produced by MCC22 and morphine in HbSS mice. **A)** Dose-response relationship for MCC22 and morphine (N=6–11 per dose). Baseline values did not differ between the groups and are therefore pooled (n=34). Mean paw withdrawal frequencies were obtained before and at 30 min following drug administration. MCC22 is shown in light gray and morphine in dark gray. **B)** Mean duration of anti-hyperalgesia produced by 8 μmol/kg (10 mg/kg) MCC22 (n=11). **C)** Mean duration of anti-hyperalgesia produced by 26.4 μmol/kg (10 mg/kg) of morphine (N = 6). * indicates a significant difference from baseline (Bonferroni t-tests; $p<0.001$).

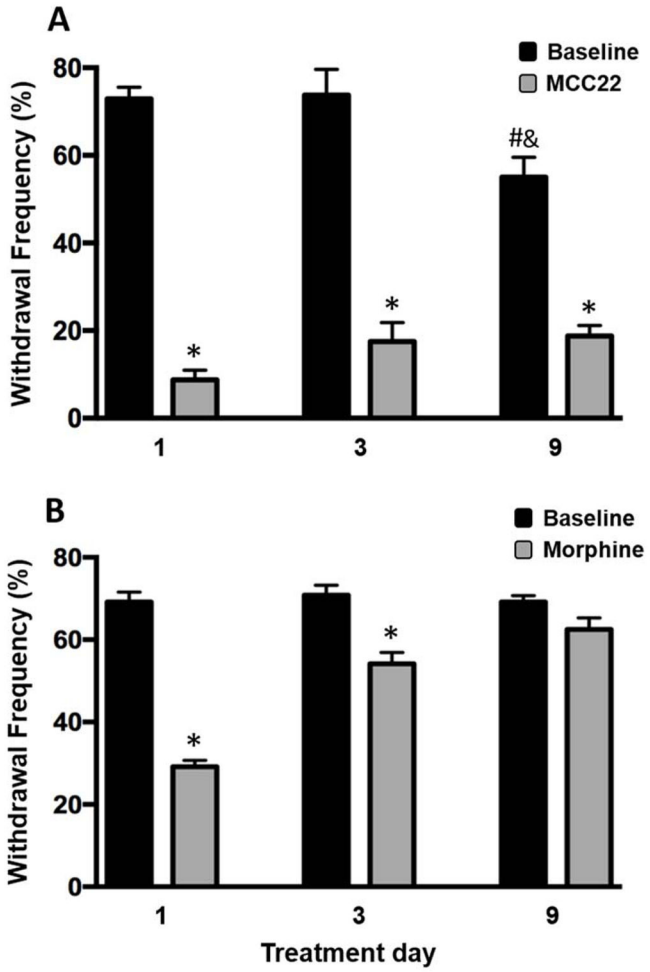

Figure 3.

MCC22 does not produce tolerance to its analgesic effect. HbSS mice were treated twice daily with i.p injections of 8 μmol/kg (10 mg/kg) MCC22 (n=8–12) **(A)** or 26.4 μmol/kg (10 mg/kg) morphine (n=6–11) **(B)** for 9 consecutive days and paw withdrawal frequency was determined before and at 30 min following the second injection on days 1, 3 and 9. No analgesic tolerance occurred in mice given MCC22 whereas complete tolerance developed in mice that received morphine. * indicates a significant difference from baseline (pre-injection) values (Bonferroni t-tests; $p<0.001$). # indicates a significant difference from day 1 baseline (Bonferroni t-tests; $p<0.001$). & indicates a significant difference from baseline day 3 (Bonferroni t-tests; $p<0.01$).

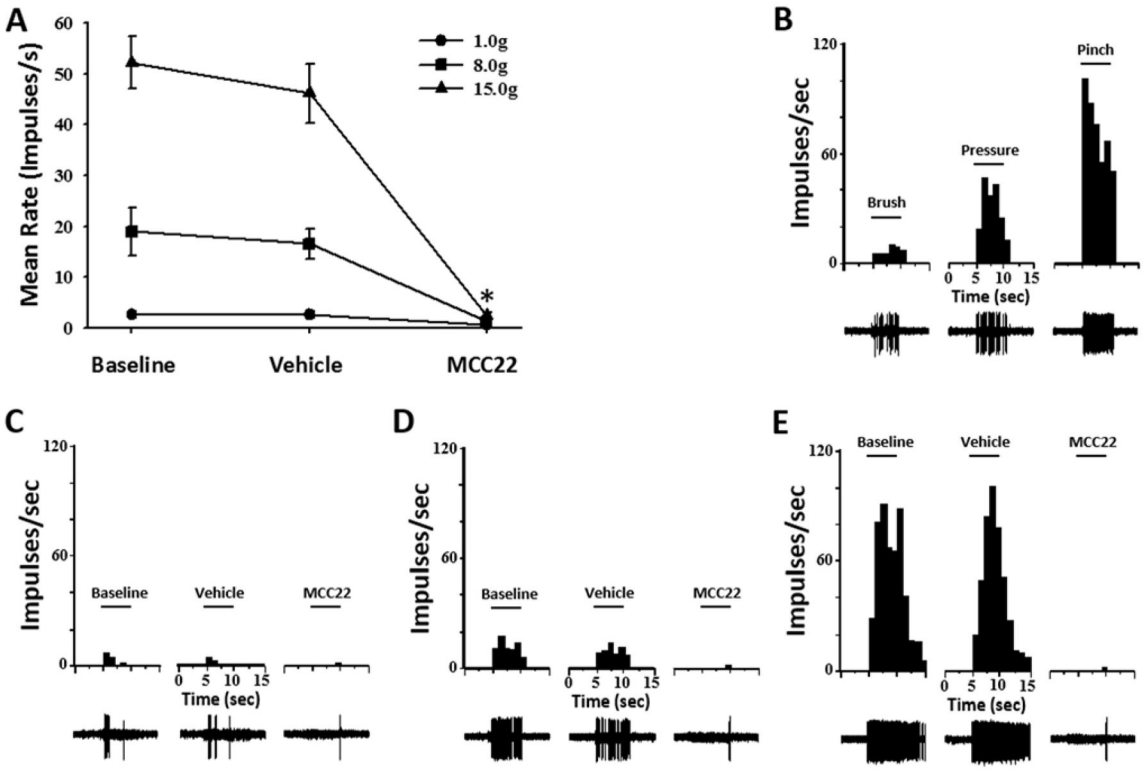

Figure 4.

MCC22 decreased responses of dorsal horn neurons evoked by mechanical stimuli in HbSS mice. **A)** Mean discharge rate (impulses/s) evoked by 1.0, 8.0 and 15.0 g von Frey monofilaments before any injection, after vehicle, and after MCC22 (8 μmol/kg; 10 mg/kg, i.p.). MCC22, but not vehicle, reduced evoked responses of nociceptive dorsal horn neurons (n=8) in HbSS mice. * indicates a significant difference from baseline (Bonferroni t-tests; $p<0.001$) for stimulus intensities of 8.0 and 15.0 g. Functional characterization **(B)** and responses (impulses/s) of a single WDR neuron evoked by 1.0 **(C)**, 8.0 **(D)** and 15.0 **(E)** g before any injection, after vehicle, and after MCC22. Response histograms show discharge rates per 1-s bin width. Evoked action potentials are shown below each response histogram.

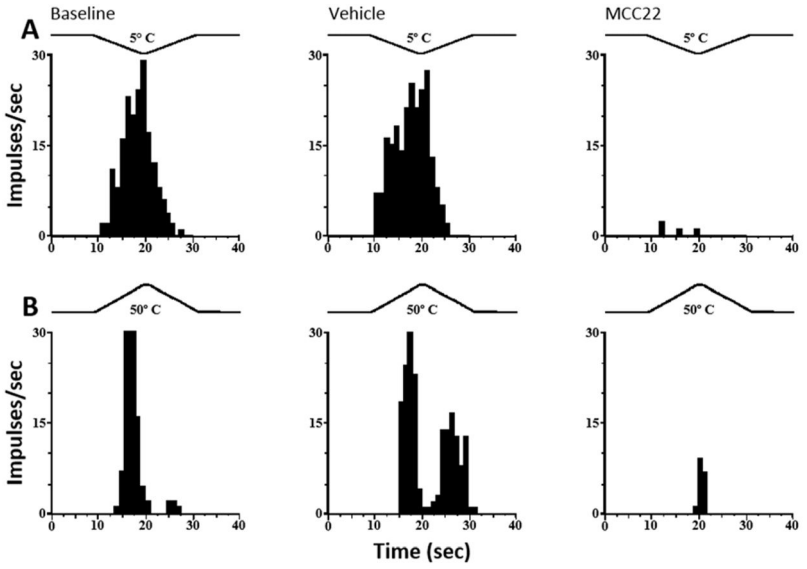

Figure 5.

MCC22 decreased responses of dorsal horn neurons evoked by heat and cold stimuli in HbSS mice. Representative examples of responses of two dorsal horn WDR neurons: **A)** Responses of a WDR neuron to heat (50° C). **B)** Responses of another WDR neurons evoked by cold (5° C). A trace of the probe temperature is illustrated above each response. Response histograms show discharge rates per 1-s bin widths. Responses to heat and cold were reduced after i.p. administration of 10 mg/kg MCC22 but not after vehicle.

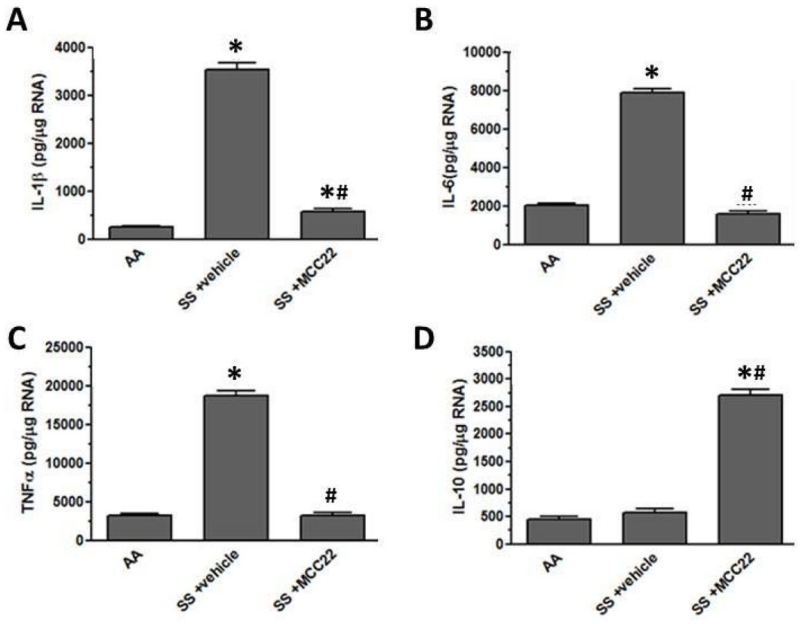

Figure 6.

MCC22 reduced pro-inflammatory cytokine and increased the anti-inflammatory cytokine IL-10 expression in the spinal cord of HbSS mice. HbSS mice were treated with i.p. injections of 8 μmol/kg (10 mg/kg) MCC22 (n=4) or vehicle (n=4) for 9 consecutive days. The spinal cord was removed from HbAA mice and HbSS mice administered vehicle or MCC22. The RNA was isolated, DNase treated, converted to cDNA, and used in real time PCR with primers for IL-1β **(A)**, IL-6 **(B)**, TNFα **(C)**, and IL-10 **(D)**. Concentrations for each cytokine were determined based on a standard set for each primer pair, and samples were normalized to β-actin expression. Significant differences in expression were determined between HbAA and HbSS vehicle-treated mice or HbSS MCC22-treated mice (Bonferroni t-tests; * $p<0.05$), and significant differences in expression were determined between HbSS vehicle-treated and HbSS MCC22-treated mice (Bonferroni t-tests; # $p<0.05$).